



Principles of Time-series SAR Interferometry

Heresh Fattahi



© 2022 California Institute of Technology. Government sponsorship acknowledged.

Acknowledgement

Thanks to:

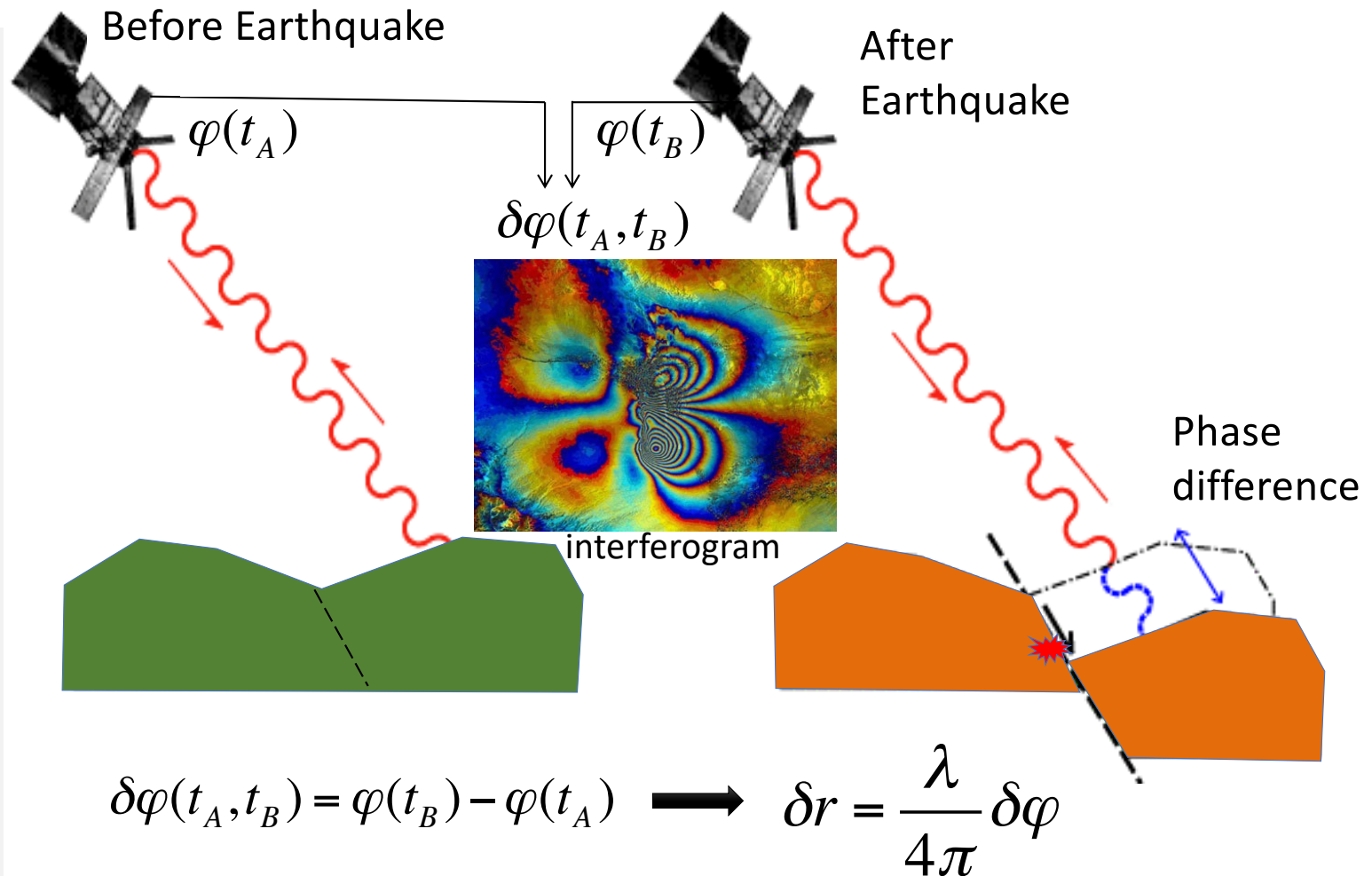
- Sara Mirzaee
- Yunjun Zhang
- Yujie Zheng
- Piyush Agram
- Falk Amelung
- Other colleagues at JPL, Caltech and University of Miami

Outline:

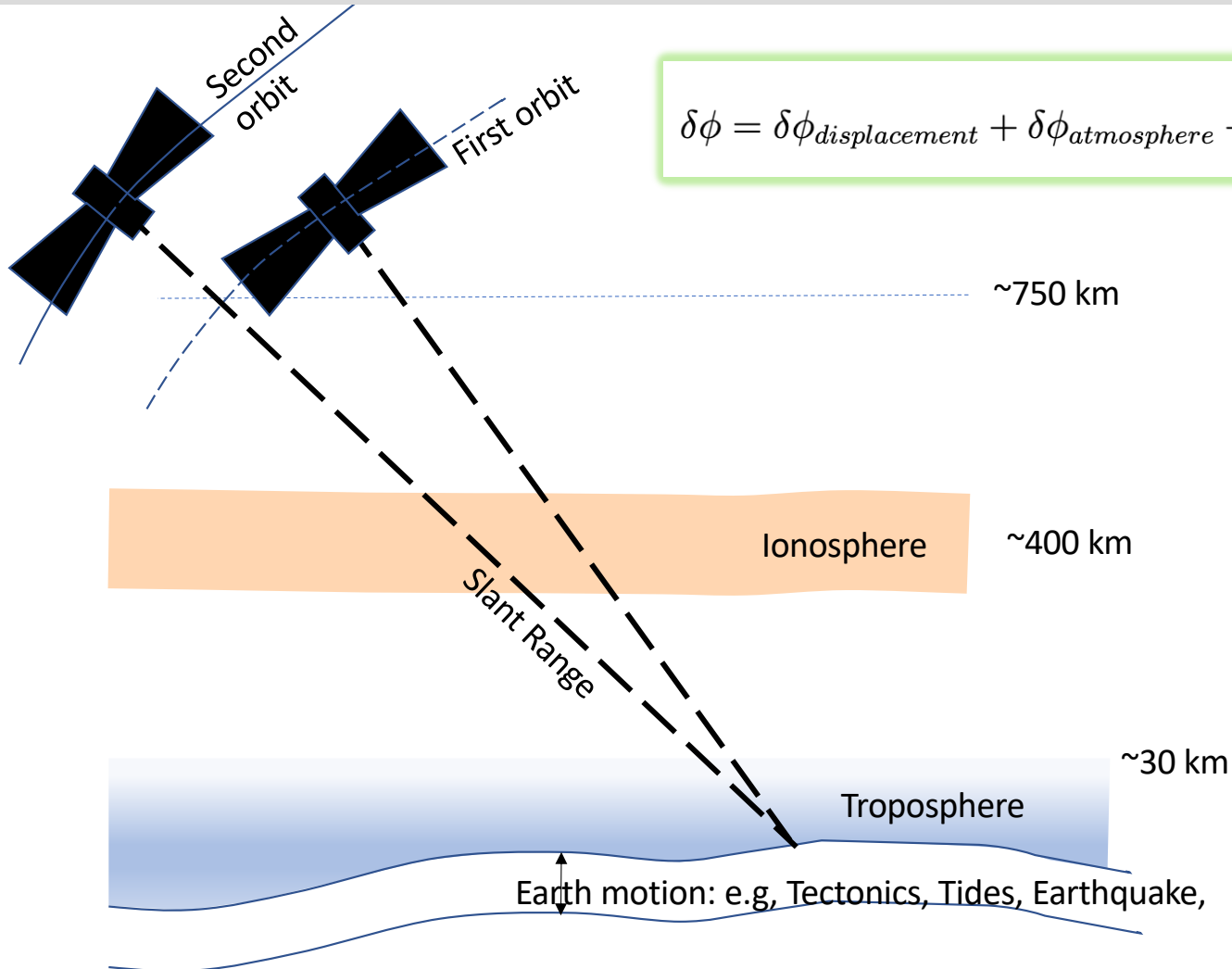
- InSAR
- Why InSAR time-series analysis?
- InSAR time-series analysis methods
 - PS timeseries
 - DS time-series
 - PS + DS
- Error analysis of the InSAR time-series
 - Propagation delay (troposphere, ionosphere)
 - DEM error
 - Unwrapping error

InSAR (Interferometric Synthetic Aperture Radar)

- InSAR is a differential technique that measures relative displacement (relative in time and space)
- InSAR measures interferometric phase, i.e., the phase difference between two SAR images acquired over the same region from the similar viewing geometry
- The phase difference is equivalent to range change or distance change between radar and target



Repeat-pass interferometric phase components



$$\delta\phi = \delta\phi_{displacement} + \delta\phi_{atmosphere} + \delta\phi_{geometry} + \delta\phi_{scattering} + \delta\phi_{noise}$$

$\delta\phi$ Total interferometric phase

$\delta\phi_{displacement}$ Surface displacement

$\delta\phi_{atmosphere}$ Atmospheric delay with contributions from ionosphere and troposphere

$\delta\phi_{geometry}$ Introduced by non-zero baseline

$\delta\phi_{scattering}$ Surface scattering components

$\delta\phi_{noise}$ Noise

Interferometric phase components

Interferometric phase components

$$\delta\phi = \delta\phi_{displacement} + \delta\phi_{atmosphere} + \delta\phi_{geometry} + \delta\phi_{scattering} + \delta\phi_{noise}$$

- **mm to cm** (tectonics, hydrological induced subsidence and uplift, tides, volcanic unrest, etc)
- 10s of cm (e.g., earthquakes)

Few cm to 10s of cm

cm

mm

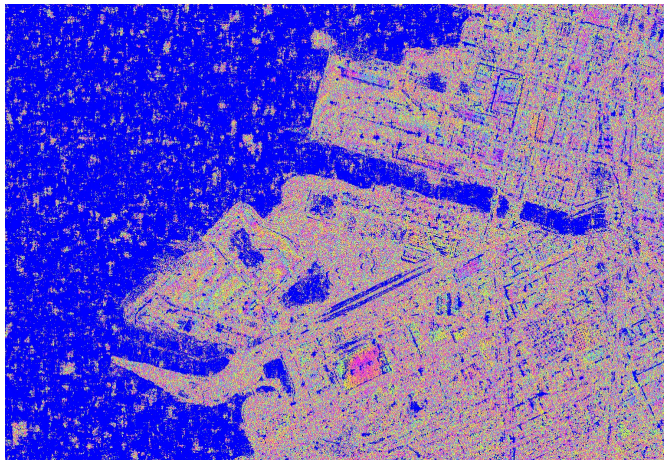
- Decorrelation (few degrees due to thermal noise up to random numbers between $-\pi$ and π for total decorrelation)
- Processing errors

- Repeat-pass interferometric data generally decorrelate with time. The longer the temporal separation between two SAR images, the noisier the interferogram is. (exceptions exist over areas with seasonal decorrelation e.g., due to snow fall, biomass change, etc. But even in those situations the background coherence reduces with time).
- For many applications with small displacement signals, the individual interferograms are dominated by atmosphere and other contributions

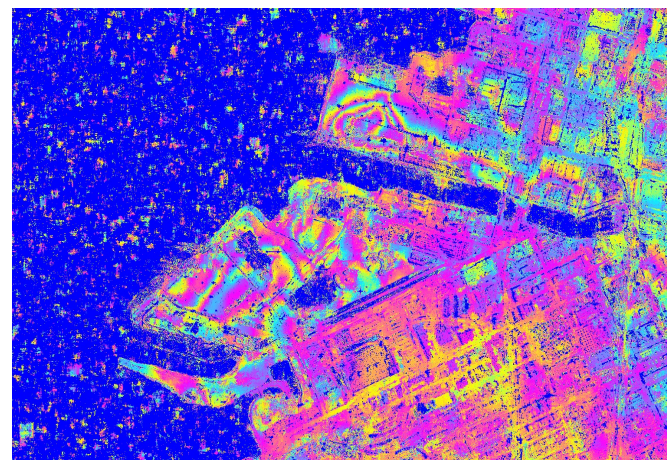
Why InSAR time-series analysis?

a. To reduce the impact of decorrelation

A regular interferogram over ~2.5 years



Same interferogram from time-series analysis



An X-band interferogram is fully decorrelated over 2.5 years



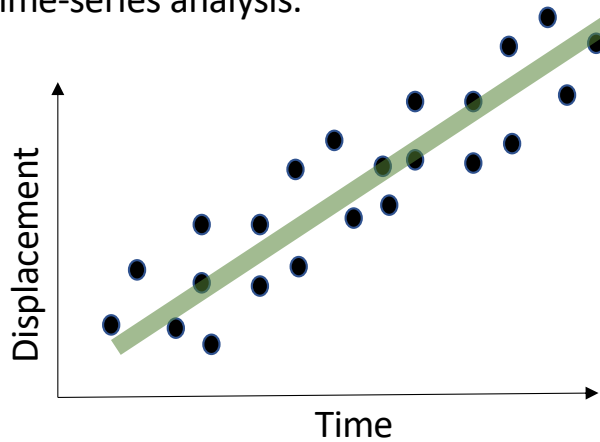
Image from Fattah, et al (JPL)

(Left) Conventional 2-pass interferometry between 2 CSK SAR scenes acquired on 2011-06-24 and 2013-10-11 over the Central Waterfront in San Francisco, CA. Subsidence features are not clear due to the large time separation between the 2 images. (Right) Interferogram generated from Sequential EVD estimator which uses the full covariance matrix in time for each pixel. Subsidence features, including sharp boundaries, are clearly preserved in this approach. The interferograms have not been corrected for troposphere and DEM error terms.

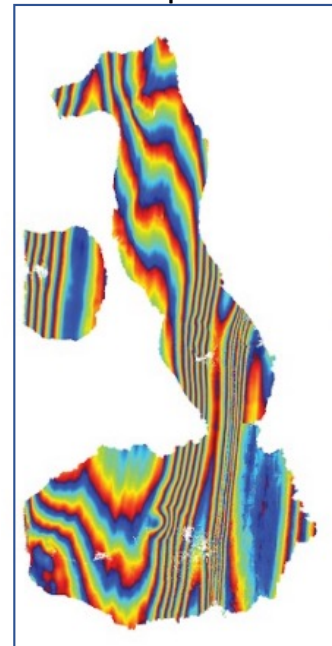
Why InSAR time-series analysis?

b. increase the accuracy of the estimated displacement signal

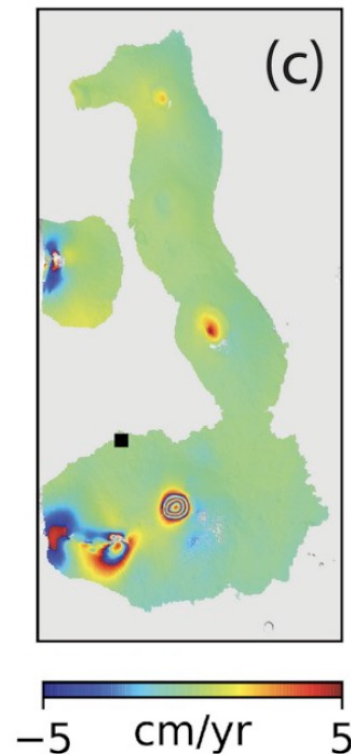
Given the ground displacement as our signal of interest, different sources of noise in the estimated InSAR displacement time-series (such as tropospheric and ionospheric delay) are mostly random in time. This temporal behavior allows to reduce the impact of noise on the estimated displacement through time-series analysis.



One interferogram
heavily dominated by
atmosphere



A velocity map derived
from time-series analysis



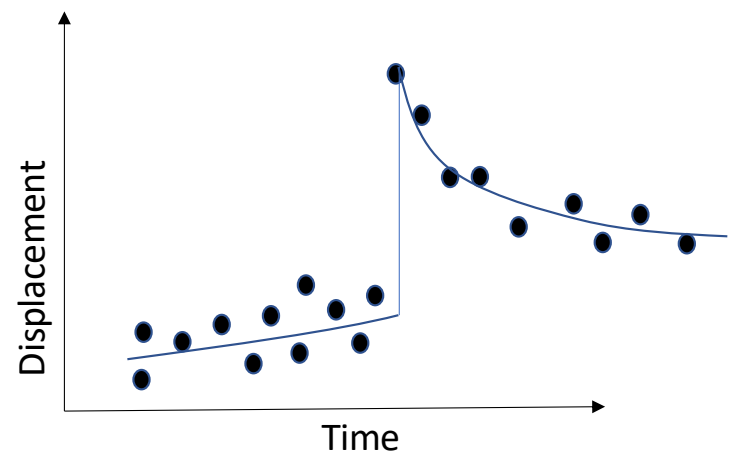
- Surface deformation due to volcanic activities in Galapagos islands are evident in the rate of displacement time-series
- The velocity field is wrapped to -5 to 5 cm/yr for visualization.

[Yunjun, Fattah, Amelung, 2019]

Why InSAR time-series analysis?

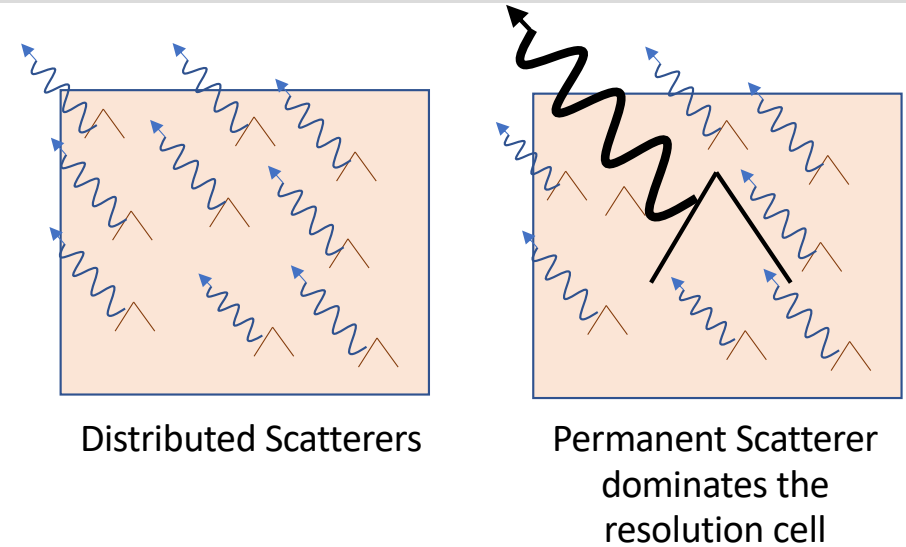
c. understand the temporal evolution of the ground displacement

- The displacement of the ground surface may evolve through time leading to non-linear change of the displacement time-series
- Examples of non-linear evolution of ground displacement:
 - Earthquake cycle (interseismic + coseismic + postseismic)
 - Volcanic unrest
 - Seasonal ground water change
- Understanding the temporal pattern of the ground displacement is crucial to better understand the driving mechanisms
- Measuring the displacement and its variation in time is only possible by time-series analysis



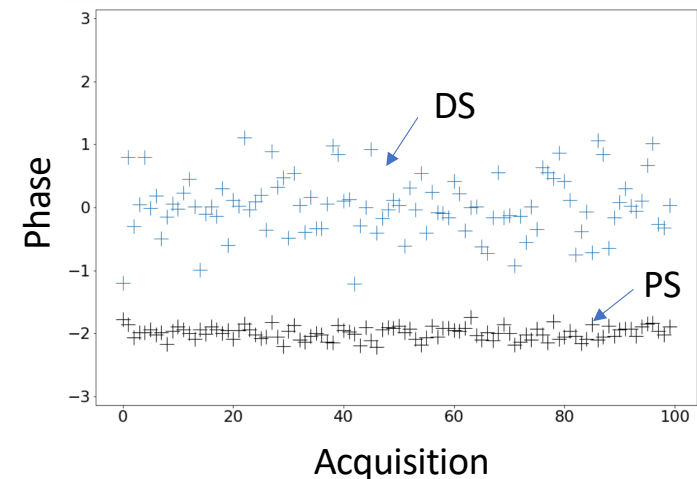
InSAR time-series analysis basics (types of Scatterers)

- One resolution cell (pixel) contains many scatterers
- A pixel may:
 - a) be largely dominated by a single point scatterer (**Persistent Scatterers (PS)**)
 - b) contain many scatterers contributing to the sum of the backscattered signal (**Distributed Scatterers (DS)**)
- The interferometric phase of PS pixels are precise over time
- The interferometric phase of DS pixels may be noisy. Therefore it is very common to reduce noise with multi-looking (averaging) many samples over a neighborhood to reduce noise



Distributed Scatterers

Permanent Scatterer
dominates the
resolution cell



Permanent Scatterer InSAR time-series analysis

PS InSAR time-series analysis involves [Ferretti et al, 2000]:

- 1- Coregister stack of SLC images
- 2- Identify PS pixels
- 3- Single-reference interferometric phase of PS pixels
- 4- Phase unwrapping an irregular grid of PS pixels

$$D_A = \frac{\sigma_{|s|}}{\mu_{|s|}}$$

$$\text{Amplitude Dispersion} = \frac{\text{Std. dev of amplitude}}{\text{Mean of amplitude}}$$

- Amplitude stability is used as a proxy for phase stability.
- Can be easily computed using a stack of coregistered SLCs.
- Works very well in urban areas.
- Can be tuned for different scattering models – e.g, two dominant scatterers etc.

PS identification has been explored in literature by adding constraints from phase stability criteria [e.g, Hooper et al 2007, StaMPS software]

InSAR time-series analysis basics (types of Scatterers)

Optical image
(Landsat/ Google)



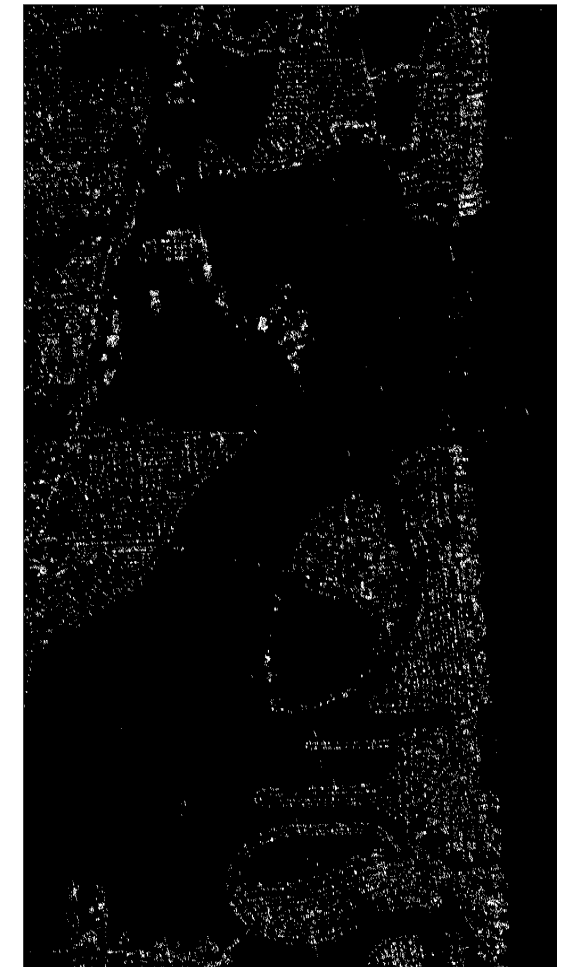
- Amplitude dispersion computed from a stack of 161 SLCs from Sep 2015 to May 2022 over north Miami beach
- Dark pixels are PS candidates
- Gray and white pixels are DS pixels

Amplitude dispersion



PS pixels

(Thresholding amp dispersion with 0.42)

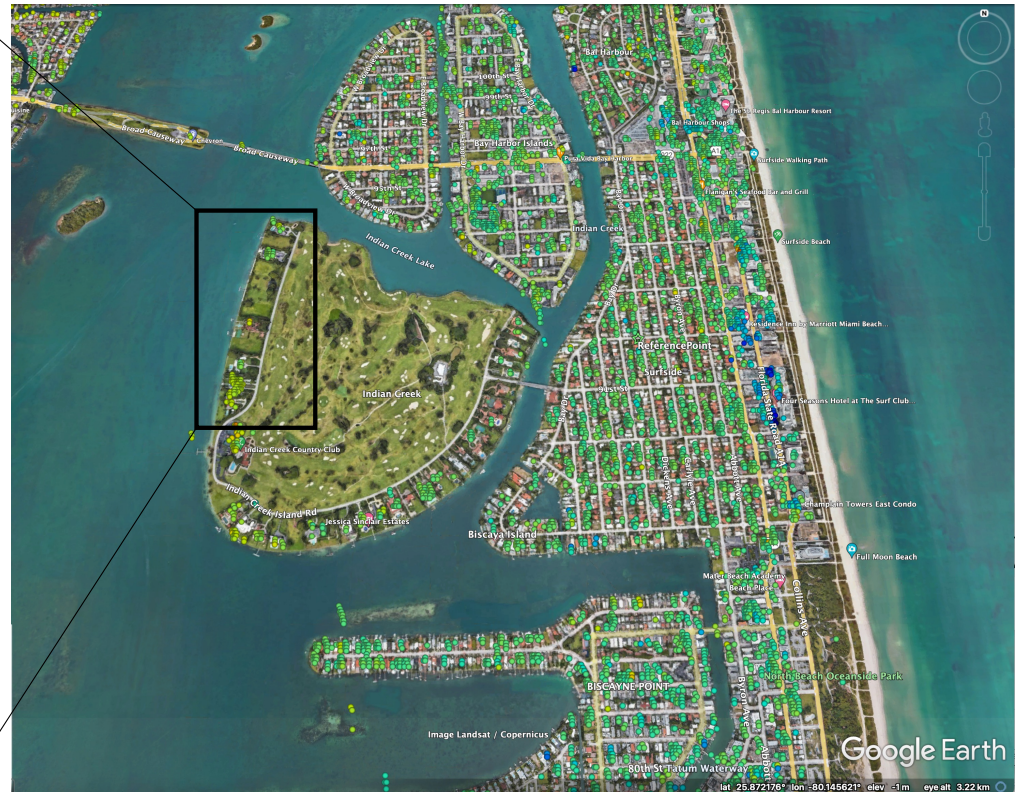


Permanent Scatterer InSAR time-series analysis



Permanent Scatterer InSAR time-series analysis

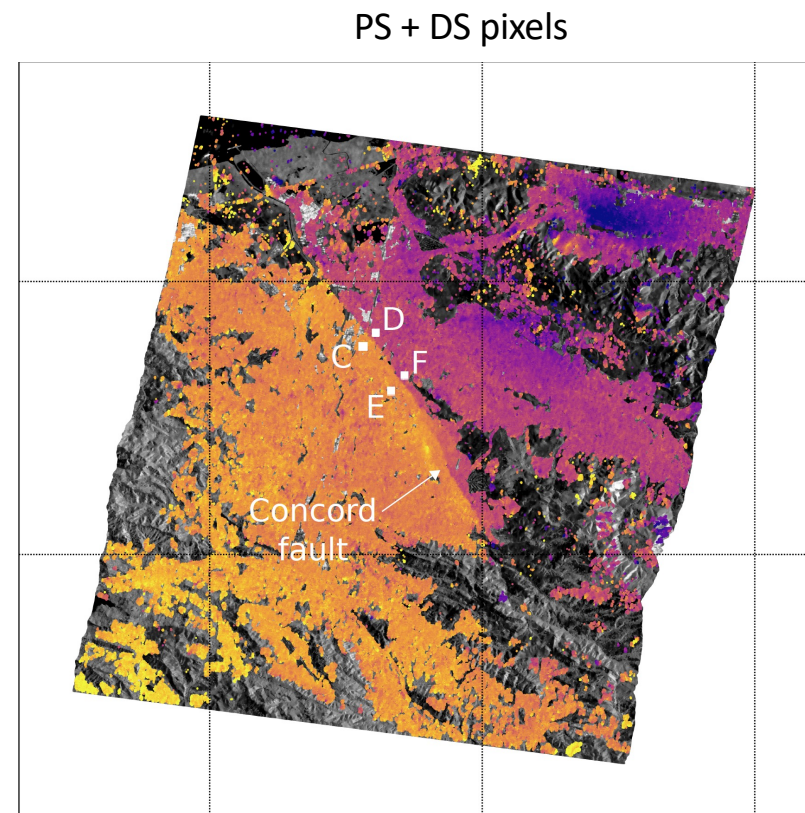
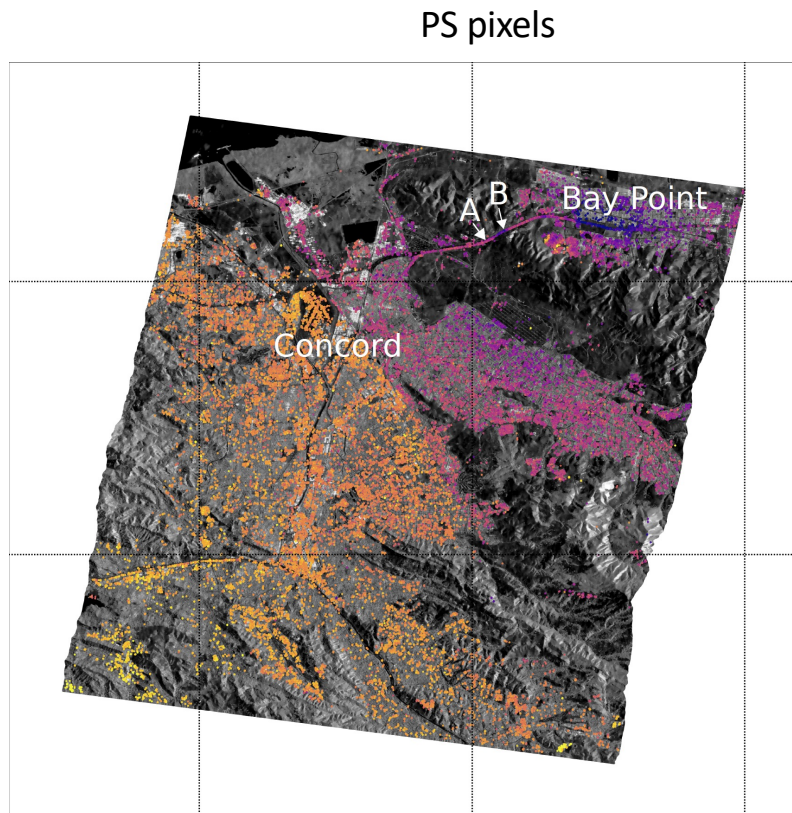
The sparse PS pixels are not easy to unwrap



Major limitations of PS algorithm:

- Although PS pixels can be easily found in urban areas, they may be rare in many natural areas.
- Phase unwrapping a low-density irregular grid of PS pixels, increases the risk of phase unwrapping errors

Permanent Scatterer InSAR time-series analysis



Higher density of pixels in the integrated PS + DS datasets will make phase unwrapping easier!

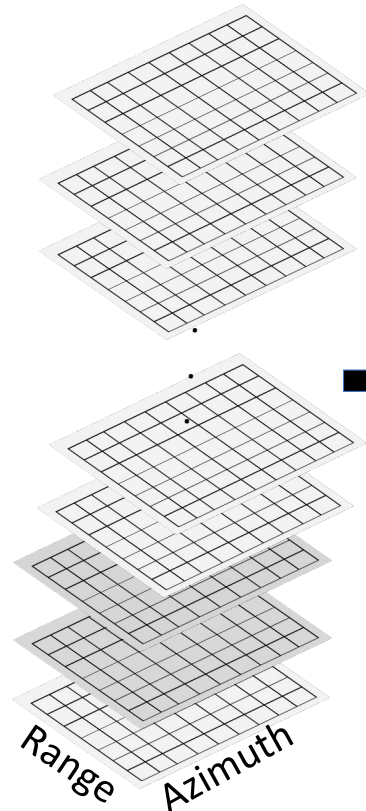
Distributed Scatterer InSAR time-series analysis (Small Baseline algorithm)

Small baseline algorithms:

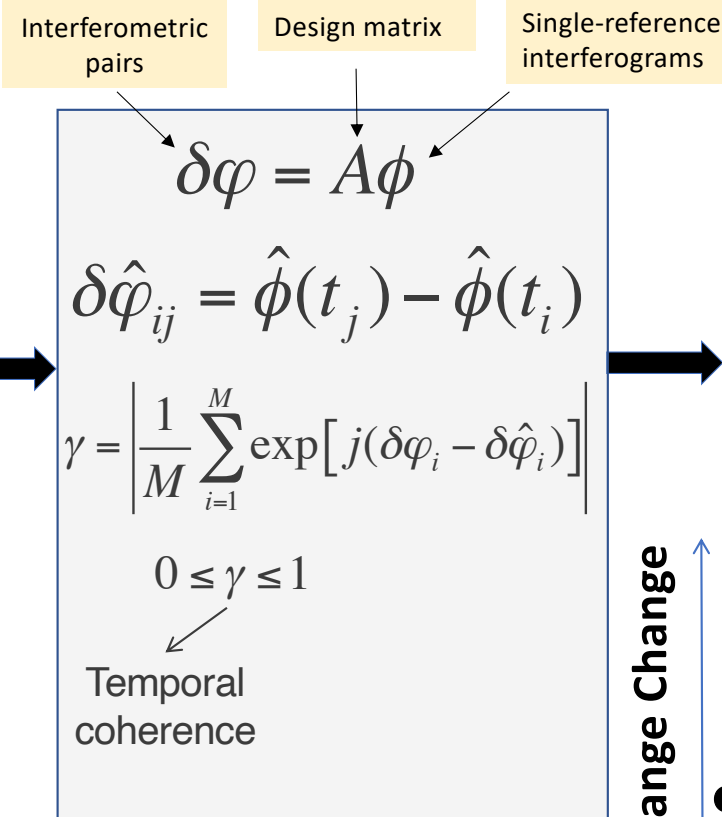
A network of interferogram pairs with small spatial and temporal baselines are formed and inverted to estimate a single network of interferograms

Small baselines ensures high coherence

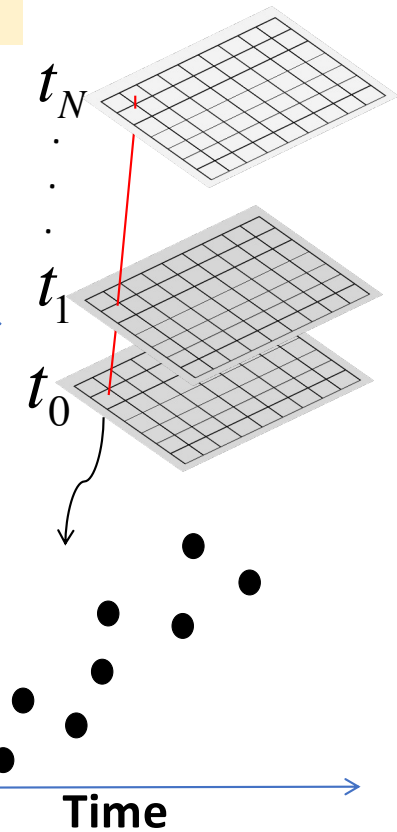
Interferograms



Inversion

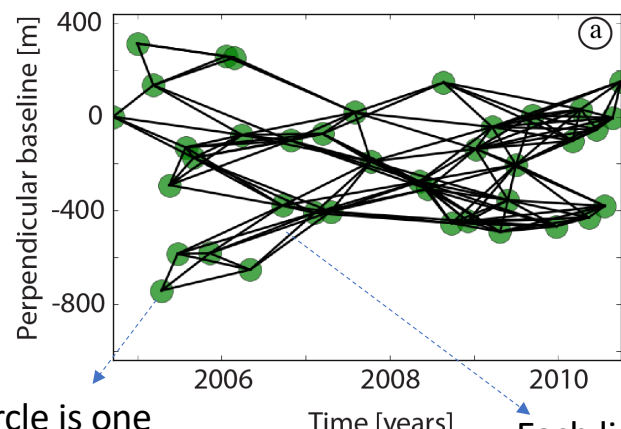


Time-series



Distributed Scatterer InSAR time-series analysis (Small Baseline algorithm)

Network of interferogram pairs

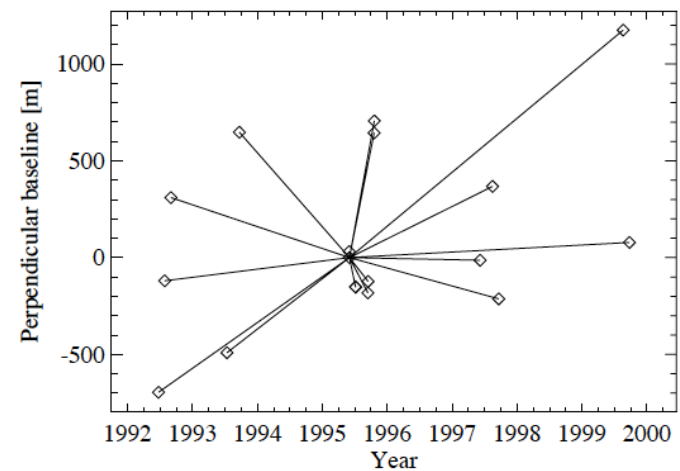


Each circle is one acquisition date (SAR image)

Each line is one interferogram

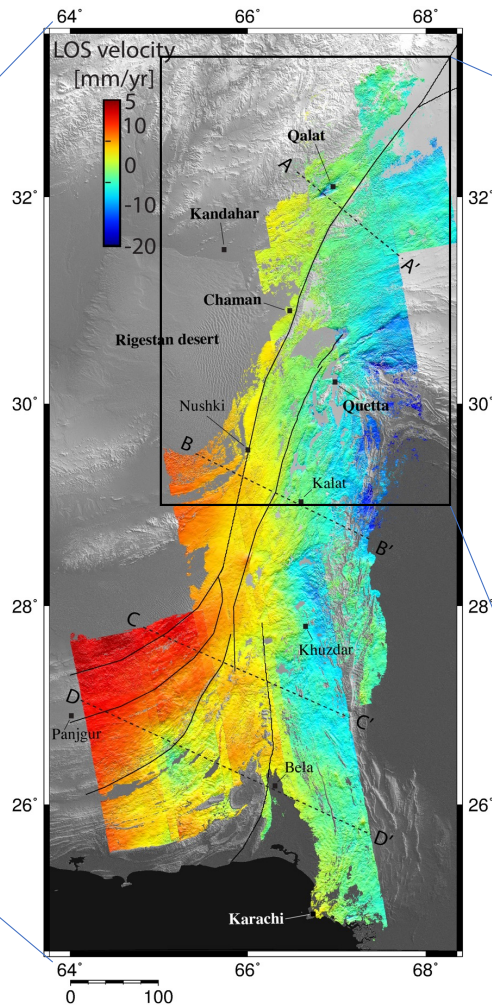
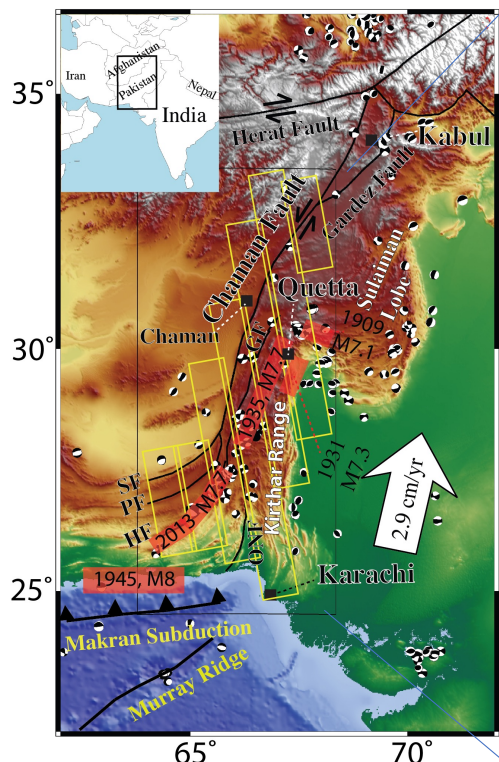
Inversion

Single reference interferograms (i.e., time-series)

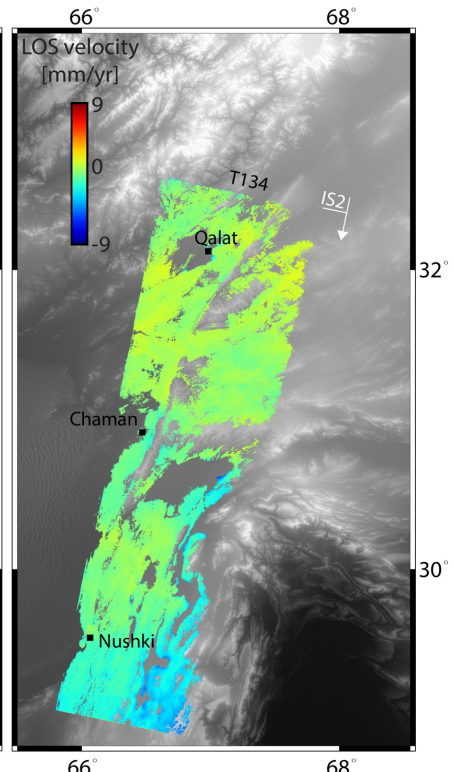
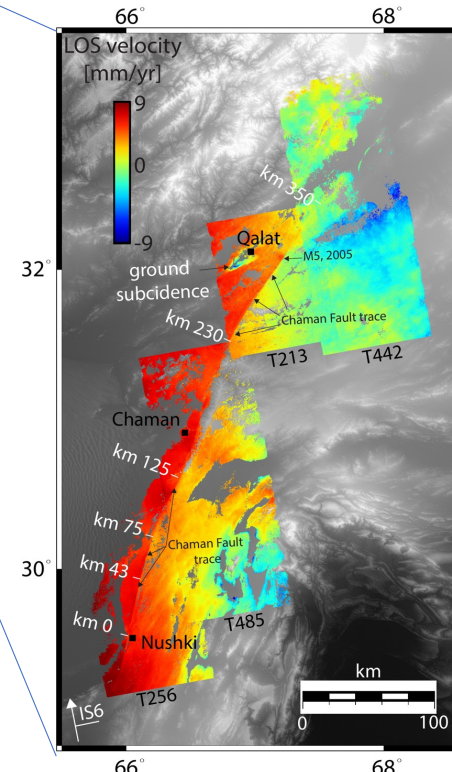


- Original Small Baseline algorithm known as SBAS was introduced by Berardino et al, 2002.
- Many other flavors of the algorithm have been introduced since then.
- Yunjun et al 2019 implemented in MintPy is an open-source Small Baseline algorithm/software.
<https://github.com/insarlab/MintPy>

Distributed Scatterer InSAR time-series analysis (Small Baseline examples)

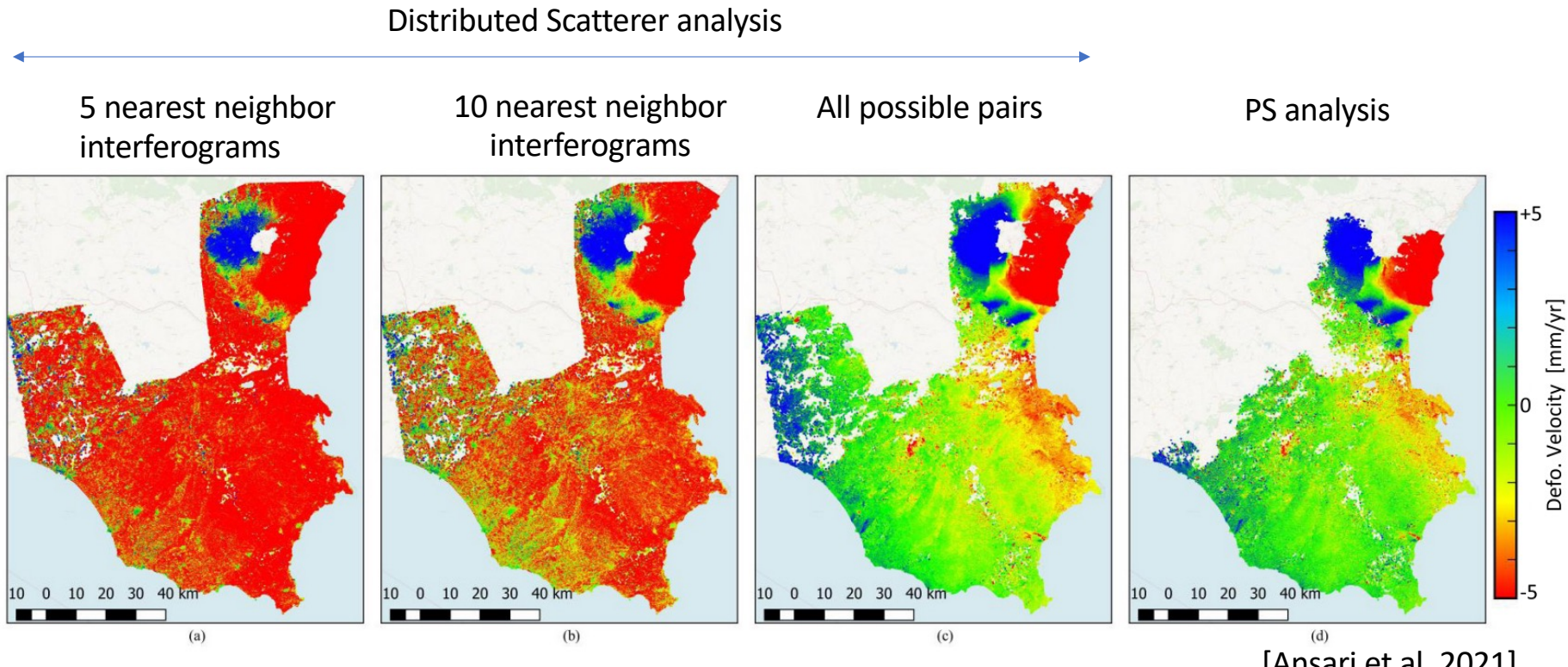


Fault creep of few mm/yr detected along the Chaman fault system



[Fattahi & Amelung, 2015]

Possible displacement bias if using only small temporal baseline interferograms



- Estimated displacement time-series over DS pixels is most accurate when all possible interferometric pairs are used.
- Using longer temporal baseline interferograms can reduce the bias (main reason why was not noticed before Sentinel-1)
- Using all possible interferometric pairs in a traditional SBAS workflow can be very expensive. An efficient approach to estimate time-series from all possible pairs is using full covariance matrix.

Phase closure as source of displacement bias

Non-closing triplets is the source of the observed bias [Zheng et al, 2022]

Phase triplet is the sum of three interferometric phases formed from three SAR acquisitions at times i, j and k

$$\Delta\phi_{ijk} = \Delta\phi_{ij} + \Delta\phi_{jk} + \Delta\phi_{ki}$$

Zero closure phase is the intrinsic assumption of all InSAR time-series analysis algorithms

For single look interferograms $\Delta\phi_{ijk} \equiv 0$ For multi-looked interferogram $\Delta\phi_{ijk} \neq 0$

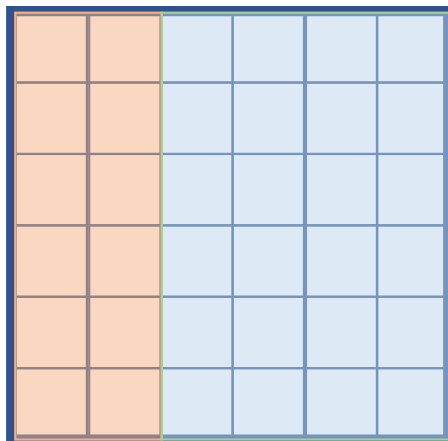
Multi-looking gives rise to non-closing triplets

Zheng et al, suggest **spatial and temporal inhomogeneity** as the source of non-closing triplet

Inhomogeneity in the multi-looking window as the source of closure phase

Multi-looking is a common practice to reduce noise over DS pixels

Window of DS pixels to average
(i.e., multi-look)



dry soil

Wet soil

The expected multi-looked signal is the weighted sum of the two groups of pixels in the multi-looking window

Assuming L independent and statistically homogeneous pixels, the multi-looked signal is given as

$$E(z) = \rho \sigma e^{i\Delta\phi}$$

Now let's assume that we have two groups of pixels. q percent of group II and $(1-q)*100/100$ percent of group I. In this case the multi-looked signal is given as

$$E(z) = (1 - q)\rho^I \sigma^I e^{j\Delta\phi^I} + q\rho^{II} \sigma^{II} e^{j\Delta\phi^{II}}$$

Assuming $w = \frac{q\rho^{II} \sigma^{II}}{q\rho^{II} \sigma^{II} + (1 - q)\rho^I \sigma^I}$

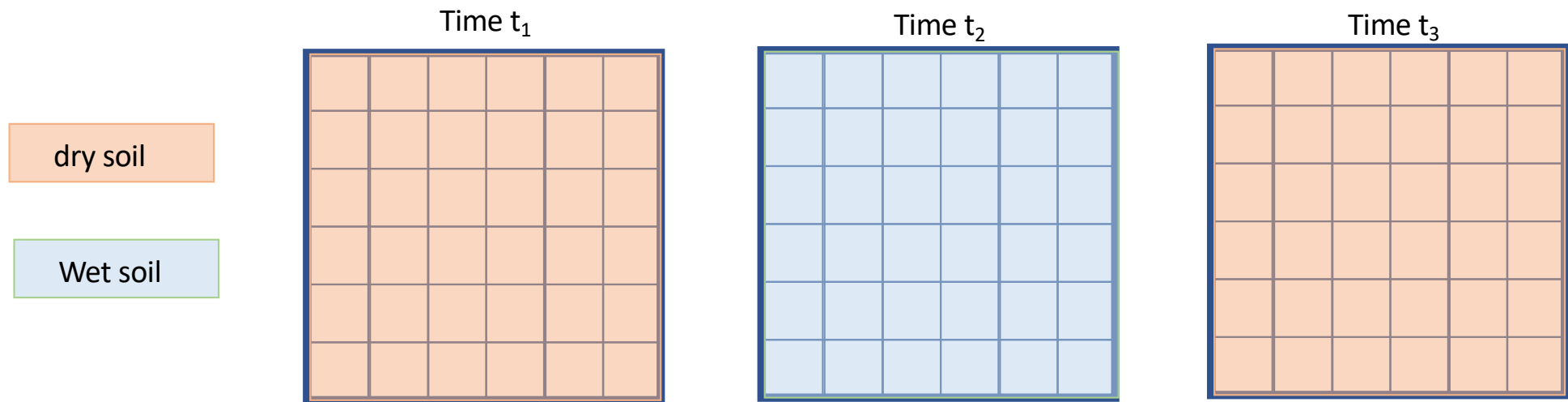
$$E(\Delta\phi) = \angle\{(1 - w)e^{j\Delta\phi^I} + we^{j\Delta\phi^{II}}\}$$

[Zheng et al, 2022]

Inhomogeneity in the multi-looking window as the source of closure phase

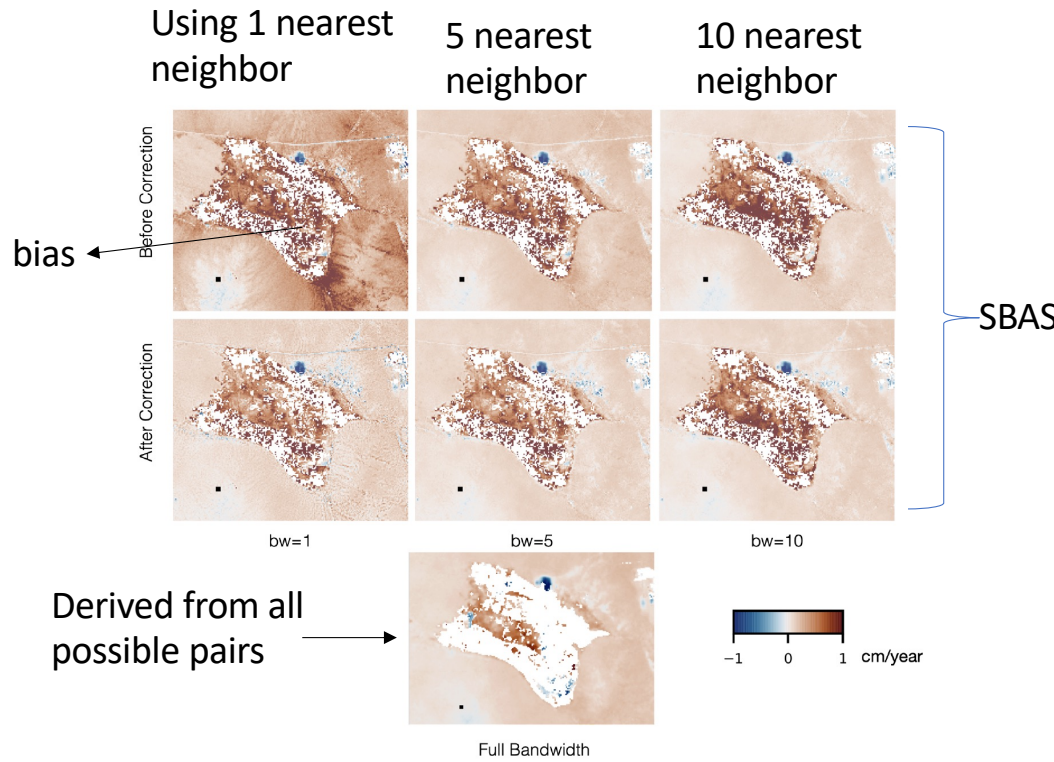
In practice it is the temporal inhomogeneity that leads to non-zero closure phase and eventually to a bias in short temporal baseline time-series

An example of temporal inhomogeneity is when the multi-looking window consists of pixels with different level of soil moisture, vegetation biomass or vegetation water content.



[Zheng et al, 2022]

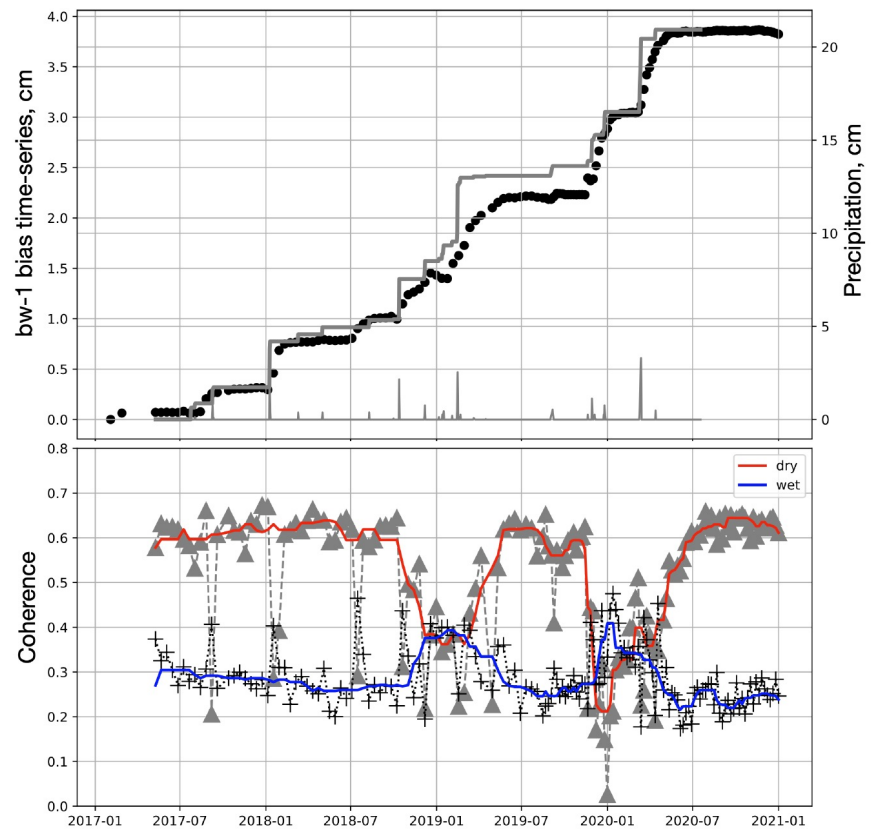
Possible displacement bias if using only small temporal baseline interferograms



How to treat the displacement bias in short temporal baseline time-series:

- 1- Use cumulative closure phase to estimate the bias
- 2- Use **all possible interferometric pairs** to minimize the bias

Estimated bias from cumulative closure phase is correlated with cumulative precipitation



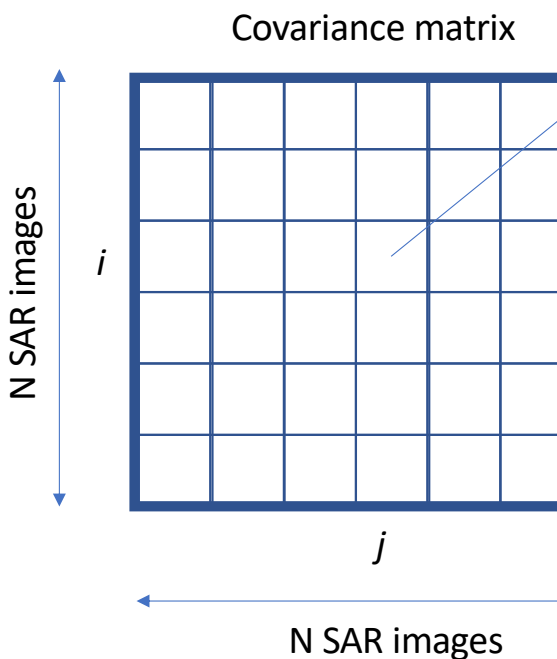
[Zheng et al, 2022]

Distributed Scatterer InSAR time-series methods (full-covariance matrix)

Covariance-based approach, extracts information from all possible interferometric phases [Guarnieri & Tebaldini, 2007 and 2008]

Assuming N co-registered SAR images, a NxN covariance matrix can be formed whose elements are multi-looked interferograms

$$\hat{C}_{ij} = \frac{1}{M} \sum_{x \in \Omega} d_x^i d_x^{j^H}$$



d_x^i A vector of complex SLCs at pixel x at time i

H Hermitian conjugate operation

Ω A neighborhood to multi-look interferometric phases

M Number of pixels in the multi-looking neighborhood

Coherence matrix is the magnitude of covariance normalized by amplitude.

$$|\Gamma_{ij}| = |\hat{C}_{ij}| / \sqrt{\sum_{x \in M} |A_x^i|^2 \sum_{x \in M} |A_x^j|^2}$$

Coherence is between 0 and 1

Full covariance based estimators for Distributed Scatterers

Given the full covariance matrix (all possible interferometric pairs), there are different algorithms to estimate the wrapped phase time-series. Following **Guarnieri and Tebaldini 2008** the time-series estimation process is referred to phase linking:

1) Maximum Likelihood Estimator (MLE) [Guarnieri and Tebaldini]:

[Ferretti et al, 2011] in the SqueeSAR algorithm, propose PTA algorithm to maximizing the probability distribution function of the data using repetitive optimization algorithms

$$\boldsymbol{\Theta} = \arg \max_{\boldsymbol{\Theta}} \{ \boldsymbol{\Theta}^H (|\hat{\Gamma}|^{-1} \circ \hat{\Gamma}) \boldsymbol{\Theta} \}$$

2) Classic Eigenvalue Decomposition (CED) [Fornaro et al 2015]

Also known as EVD or CEASAR, the CED estimator suggest that the phase of the eigenvector corresponding to the largest eigenvalue of the complex covariance matrix represents the wrapped phase time-series

$$\hat{\Gamma} \hat{\boldsymbol{v}} = \lambda_m \hat{\boldsymbol{v}}$$

3) Eigenvalue Based Maximum Likelihood Estimator (EMI)

Instead of using PTA for estimating the MLE of the wrapped phase time-series. [Ansari et al, 2018] suggest to simply take the eigenvector corresponding to the minimum eigenvalue of $|\hat{\Gamma}|^{-1} \circ \hat{\Gamma}$

$$(|\hat{\Gamma}|^{-1} \circ \hat{\Gamma}) \hat{\boldsymbol{v}} = \lambda_m \hat{\boldsymbol{v}}$$

Full covariance based estimators for Distributed Scatterers

Simulations show that MLE estimates of wrapped phase time-series are more precise than the CED estimates

However, MLE estimators require computing the inverse of the Coherence matrix. Computing the inverse requires the coherence matrix to be positive-definite.

Ignoring an estimate when coherence is not positive definite will lead to loosing an estimate for many coherent pixels.

4- Combined phase-linking algorithm [Mirzaee, Amelung, Fattah, 2022, in review]:

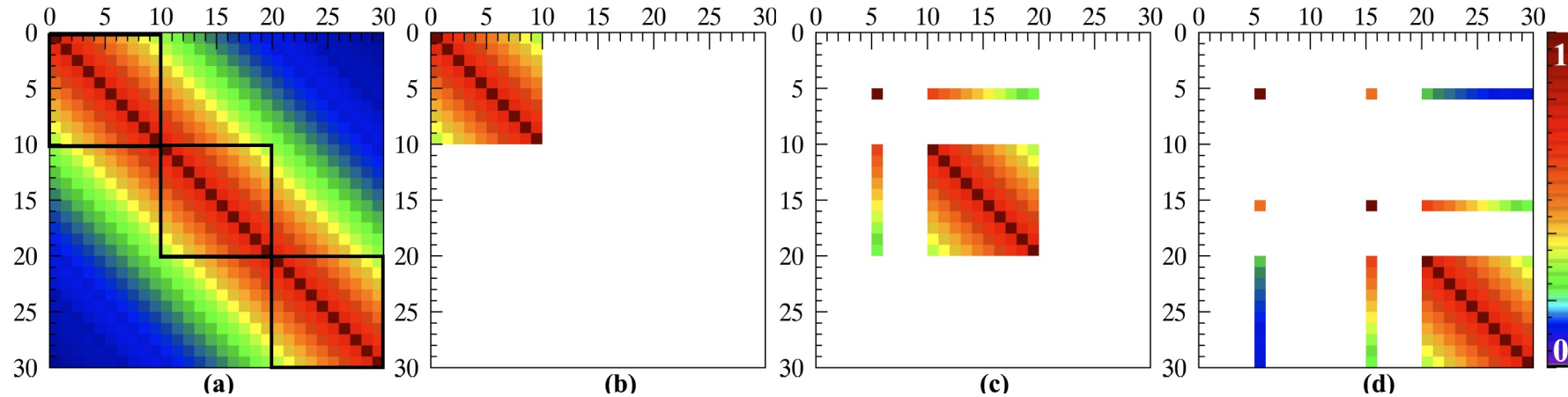
- 1- Compute Covariance and Coherence matrices
- 2- Check if Coherence is positive
- 3- If Coherence is positive-definite, Estimate MLE
else:
 - Regularize Coherence
 - if regularized coherence positive-definite, estimate MLE
 - else estimate CED

Big-data problem for full covariance based estimators

Regardless of the choice of the estimator, the wrapped phase time-series from a full covariance matrix formed from a large stack of SLCs is an expensive operation.

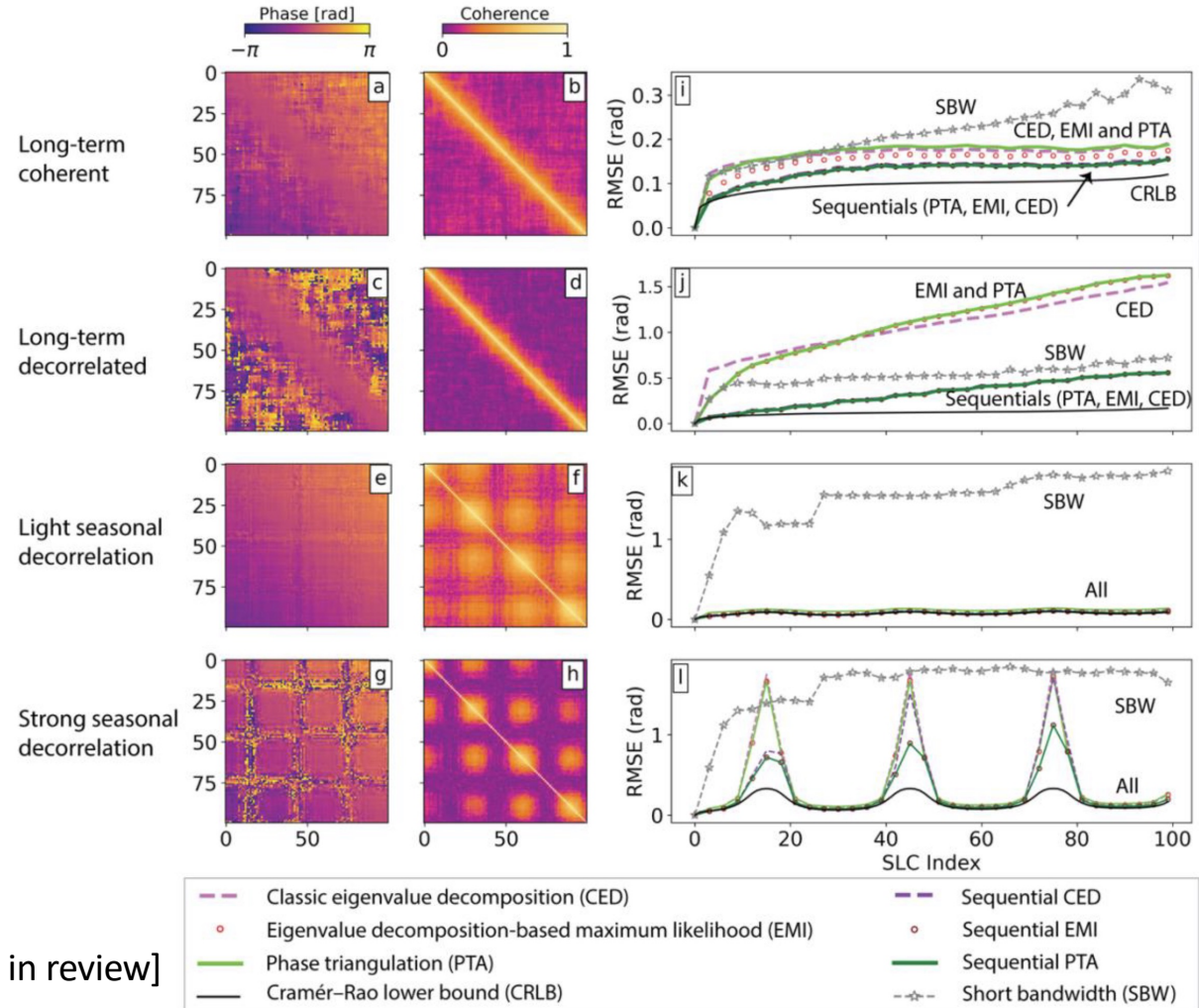
With new acquisitions added to the existing stacks, there is a need for time-series update in opposite to reprocessing the entire stack with every new acquisition.

Ansari et al, 2017 proposed Sequential Estimator algorithm which processes a covariance matrix in batch and allows to update an existing time-series without processing the full covariance matrix.



Full covariance-based estimators for Distributed Scatterers

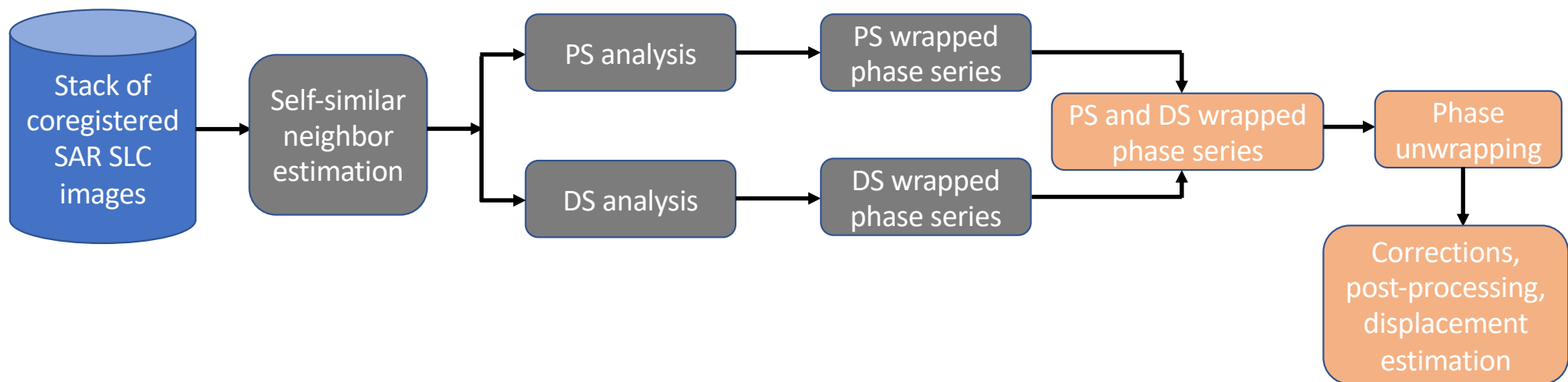
- A simulation to compare the precision of the different estimators assuming different decorrelation models
- With 1000 realizations the simulation shows that in general:
 - Sequential estimator is an optimum estimator
 - EMI is more precise than CED
 - Short temporal baseline can NOT handle seasonal decorrelation



[Mirzaee et al, 2022, in review]

PS+DS Scatterer InSAR time-series analysis

The workflows that combine PS and DS pixels follow the following general flow:

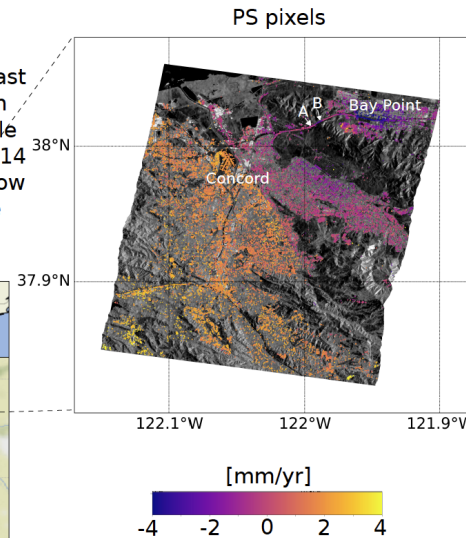
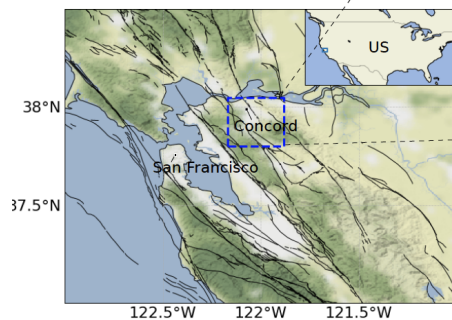


- Integrating DS and PS pixels, increases the density of pixels in the estimated wrapped phase time-series and makes phase unwrapping easier
- Multi-looking over **self-similar neighbors**, preserves fine features in the DS time-series results

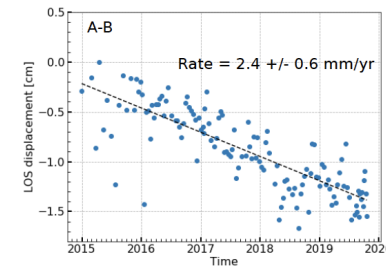
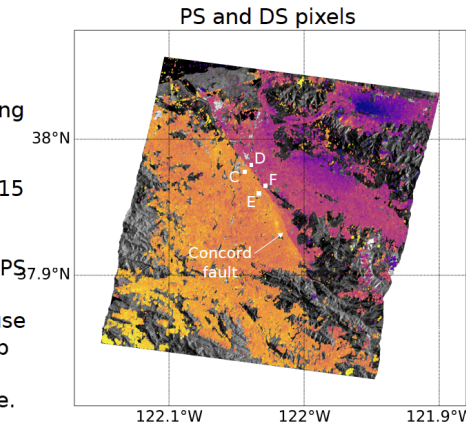
PS+DS InSAR time-series analysis (Examples)

Example 1: Concord Fault

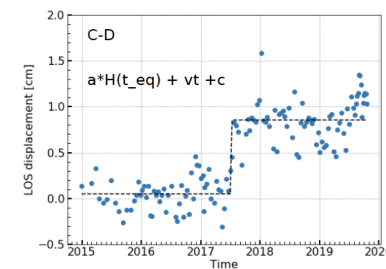
Concord fault, a strike-slip fault running through Concord city, California in the east of San Francisco bay area is under a high stress level and therefore may be capable of producing earthquakes larger than 2014 South Napa earthquake (USGS). At shallow depths, the fault may release part of the strain aseismically with episodic events.



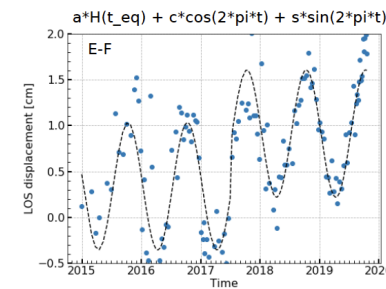
138 SAR acquisitions acquired by Sentinel-1 were coregistered using ISCE. We estimated the neighborhood map using KS2 test and the estimated the wrapped phase time-series of DS pixels using the Sequential approach with mini-stacks of 15 acquisitions and with the eigen-decomposition as the solver. We used an amplitude dispersion of 0.4 for choosing PS pixels and then unwrapped the phase series of PS and DS pixels together. We use 2D unwrappers to simultaneously unwrap the PS and DS pixels. The DS and PS rate maps generally agree.



Strong
subsidence
signal



A creep event

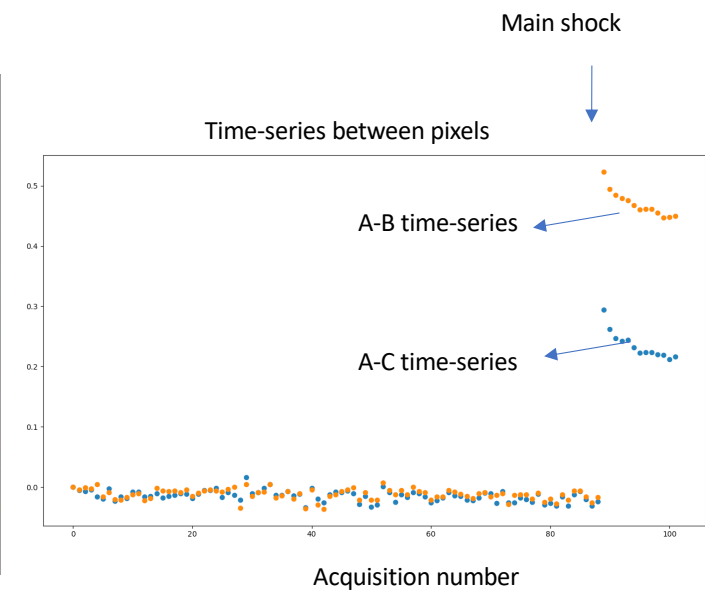
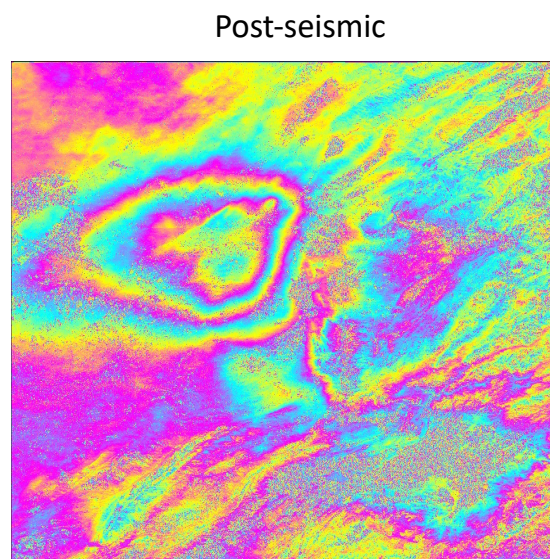
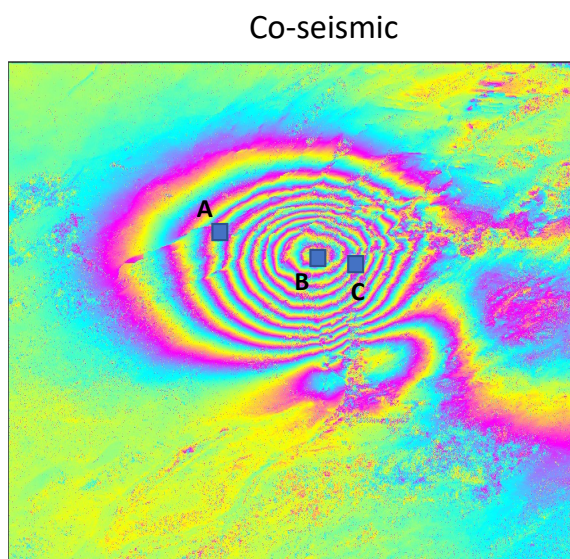


Seasonal
displacement
superimposed
on the creep
event

[Fattahi et al, 2019]

PS+DS InSAR time-series analysis (Examples)

Kurdistan Earthquake, 2017



- A stack of 120 coregistered SLCs were processed with full covariance algorithm (using FRInGE) to estimate the wrapped phase time-series.
- The wrapped phase time-series were unwrapped.
- The co-seismic and post-seismics are the result of a fit to the estimated unwrapped time-series

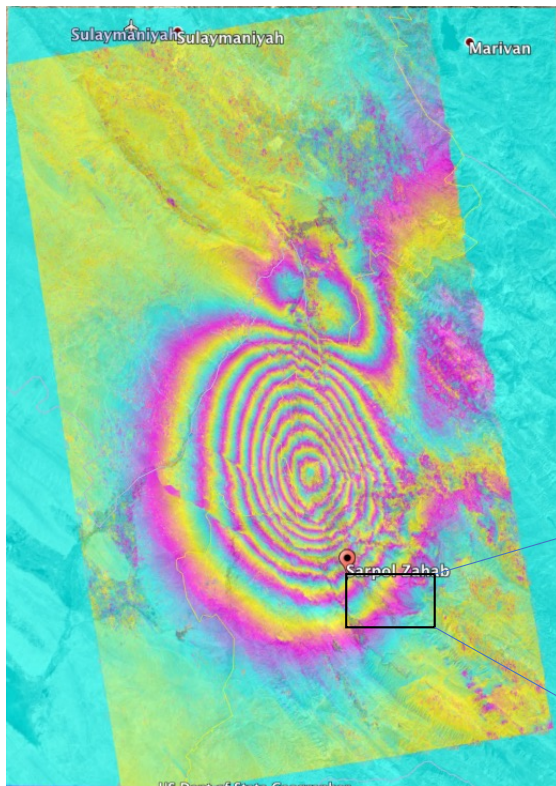
PS+DS InSAR time-series analysis (Examples)

Magnitude of the normalized full covariance matrix, represents the coherence matrix

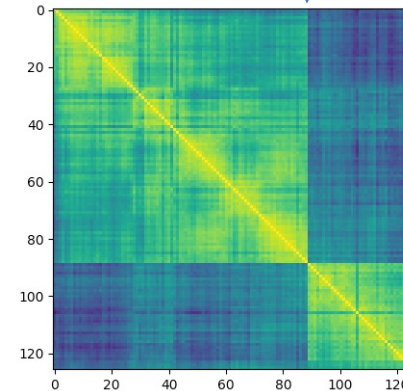
Changes in the scattering properties of the scene can impact coherence

Changes can be potentially detected by coherence time-series

Co-seismic



A change in the coherence magnitude history most likely caused by the damages caused by the Earthquake

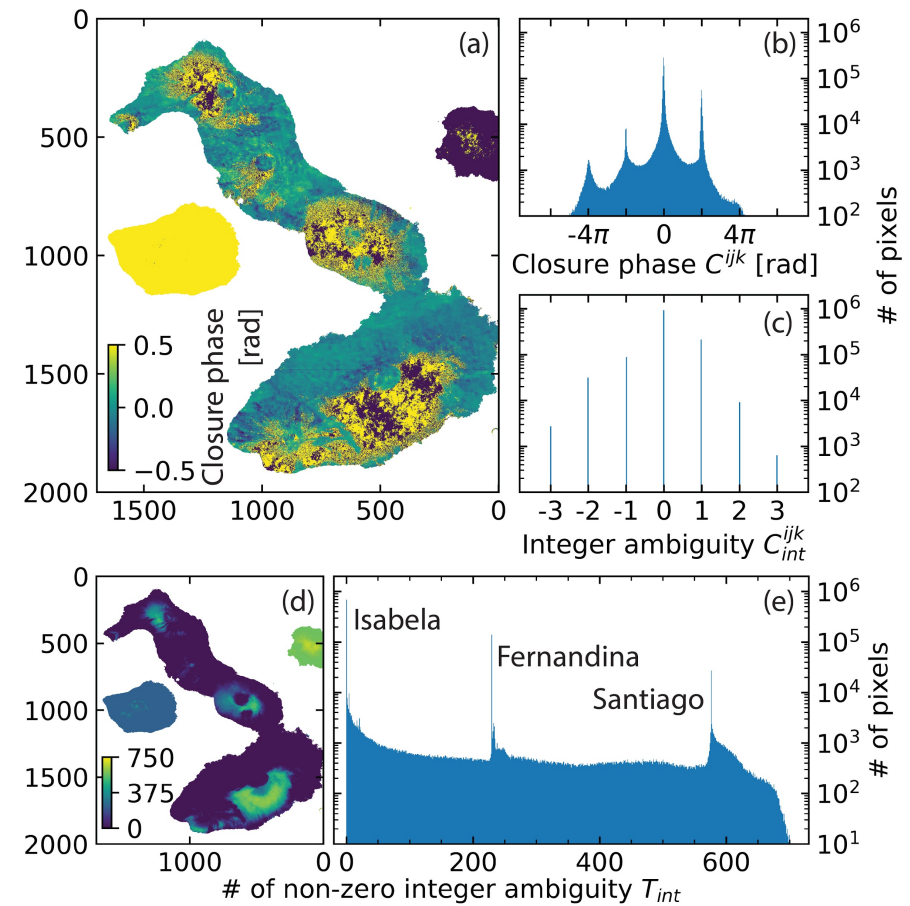


A change in the coherence matrix after the earthquake, demonstrates the potential of full coherence matrix for change detection and damage proxy mapping.

Error analysis of the estimated displacement timeseries

Phase Unwrapping errors

- Phase unwrapping is the process of reconstructing the phase field by adding integer number of phase cycle to the wrapped interferometric phase
- Unwrapping error: wrong integer cycle (wrong 2π) added to the wrapped phase
- Unwrapping errors can lead to non-closing triplets of the Integer cycles
- Evaluating the closure phases of the dense stacks of interferograms helps to identify areas affected by unwrapping errors and potentially correct them



Yunjun et al (2019)

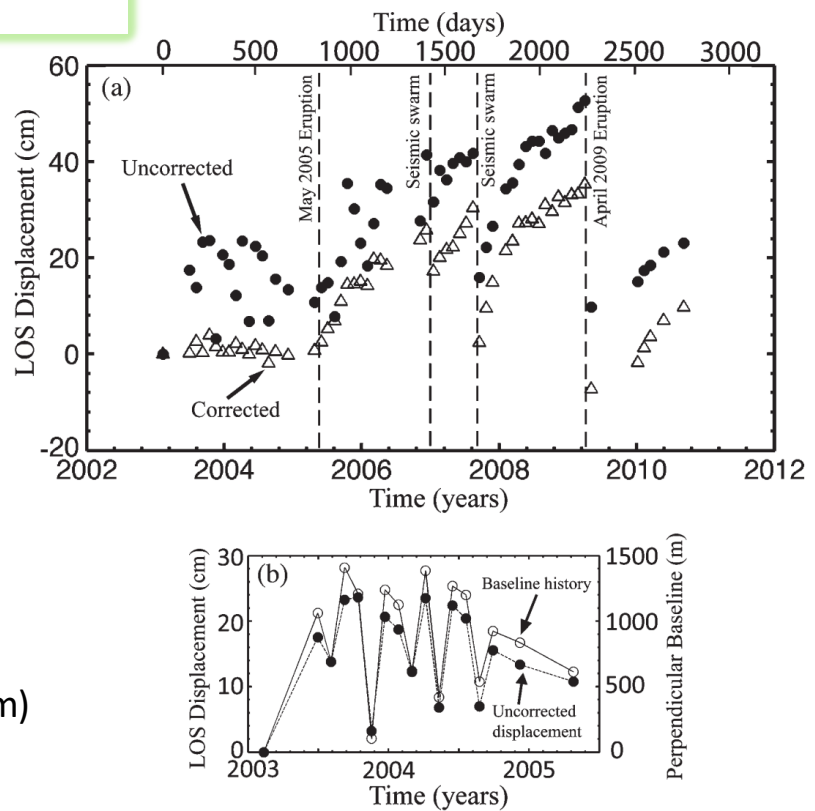
Impact of DEM error on InSAR time-series

$$\delta\phi = \delta\phi_{displacement} + \delta\phi_{atmosphere} + \delta\phi_{geometry} + \delta\phi_{scattering} + \delta\phi_{noise}$$

- We use an existing Digital Elevation Model (DEM) to remove topographic component from the interferometric phase.
- Any error in DEM will lead to residual topographic effects in the estimated time-series
- The contribution of DEM error in the estimated time-series is a function of the perpendicular baseline time-series. This dependency allows to estimate DEM error from InSAR time-series data when the baseline diversity increases the sensitivity to DEM errors

$$\phi_{topo}^{\varepsilon}(t_i) = \frac{4\pi}{\lambda} \frac{B_{\perp}(t_i)}{r \sin(\theta)} z^{\varepsilon}$$

- Sentinel-1 and NISAR have small baseline variation (< few hundred m) and therefore are less sensitive to DEM errors
- Missions with large baseline diversity (e.g, CSK Envisat, ERS, ALOS-1) with few km baseline separation, are most affected by DEM error.



[Fattah & Amelung, 2013]

Impact of Tropospheric delay on InSAR time-series

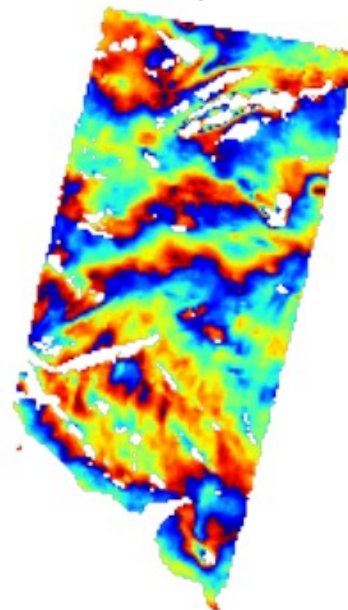
$$\delta\phi = \delta\phi_{displacement} + \delta\phi_{atmosphere} + \delta\phi_{geometry} + \delta\phi_{scattering} + \delta\phi_{noise}$$



- Microwave signals experience a delay while propagating through atmosphere.
- The two main components of the delay comes from **troposphere** and **ionosphere** layers of the atmosphere

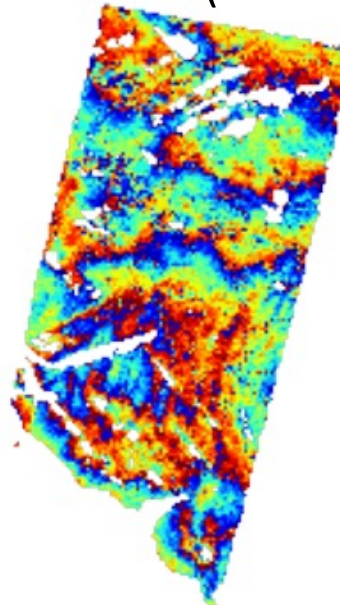
In this example independent observation from optical sensor (MERIS) acquired at the same time as the SAR acquisition predicts the impact of tropospheric delay on InSAR data

InSAR



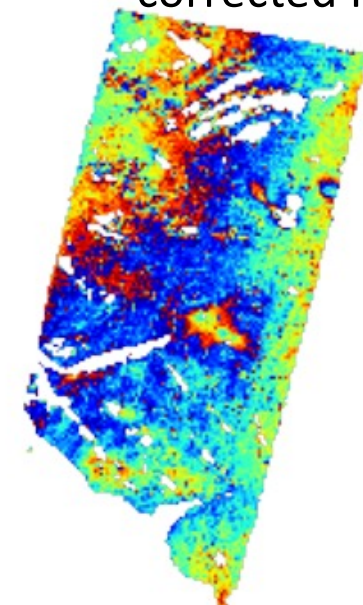
30 m x 30 m

MERIS (wet delay)



1.6 km x 1.6 m

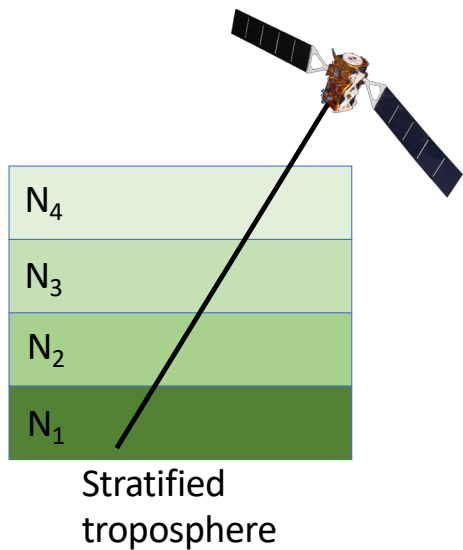
corrected InSAR



[Fattah 2015]

Tropospheric delay

Atmospheric delay is the integral of air refractivity between the ground and the satellite.



Refractivity

$$N = (n - 1)10^6$$

Tropospheric delay =

$$N = k_1 \frac{P_d}{T} + k_2 \frac{e}{T} + k_3 \frac{e}{T^2}$$

dry delay

wet delay

e: Water vapor partial pressure

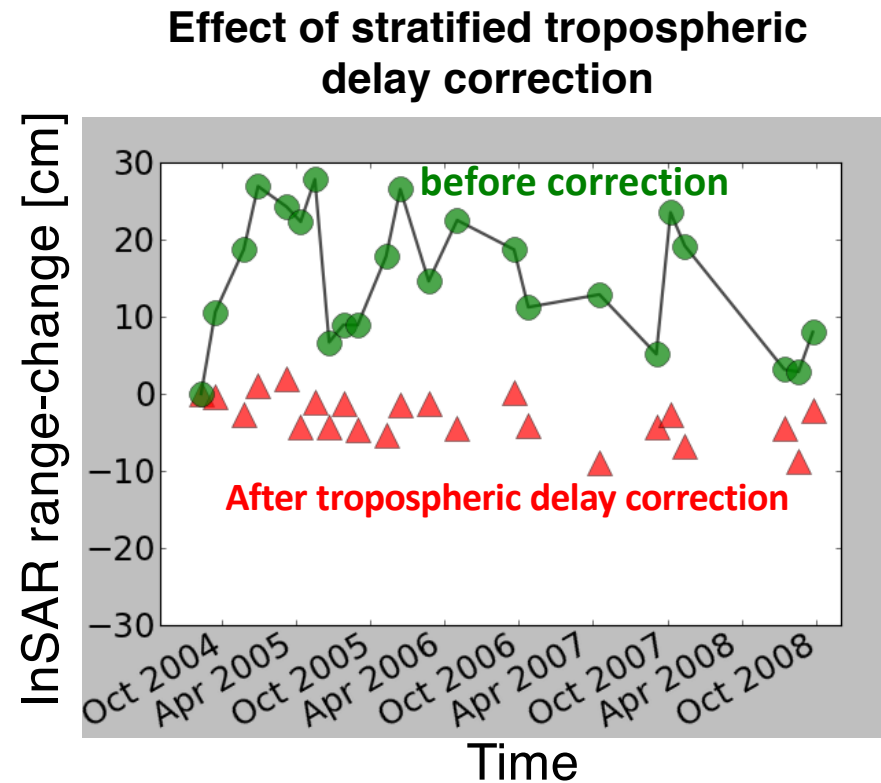
T: temperature

P_d: dry air pressure

Usually 80% to 90% of the delay is wet delay

Tropospheric delay

- The time-series between two pixels ~200 km away in western Indian plate boundary, significantly improves after tropospheric delay correction.
- The tropospheric delay correction using atmospheric models depends on the spatial resolution of the model, their temporal sampling and accuracy of the model parameters
- The tropospheric delay correction using atmospheric models usually can NOT correct the turbulent component of the delay

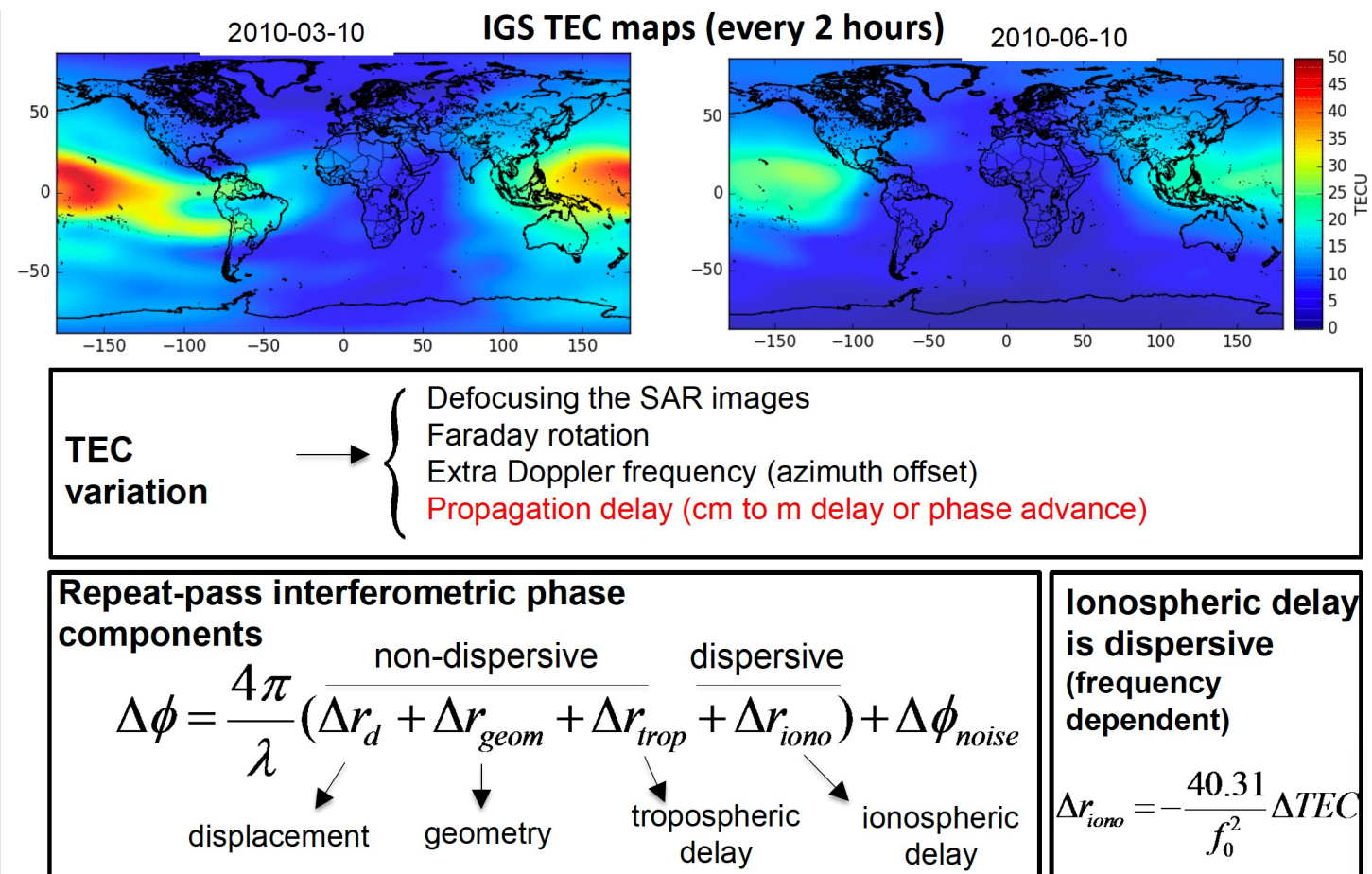


Ionospheric phase

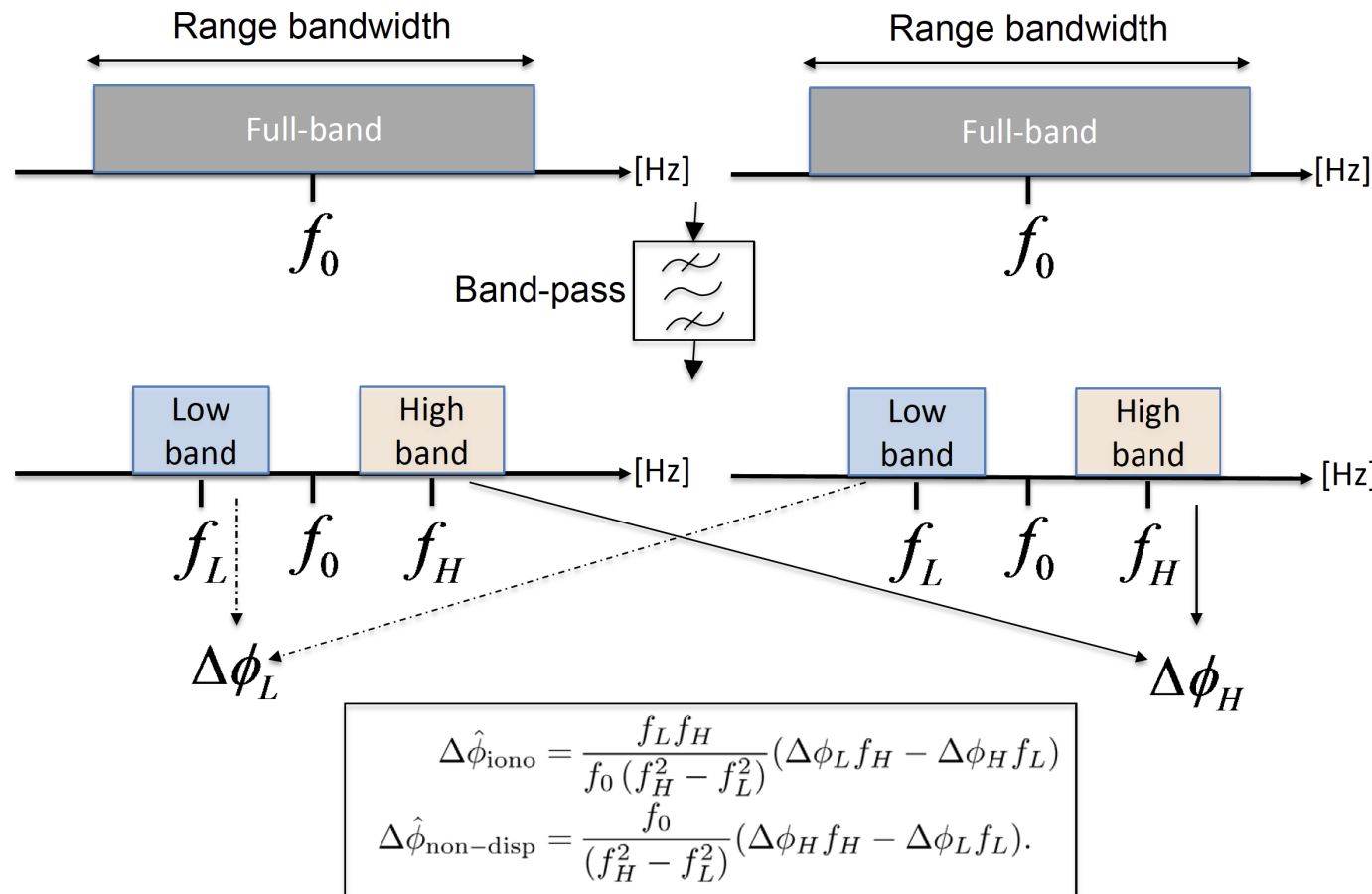
Ionosphere is a dispersive media with respect to microwave signal

Ionosphere impacts SAR data in all different frequencies. However the effect is larger in low frequencies (e.g., P and L bands compared to high frequencies such as X and C bands)

The dispersive nature of ionosphere provides an opportunity to estimate the ionospheric delay from SAR data



Ionospheric phase estimation (split range-spectrum technique)

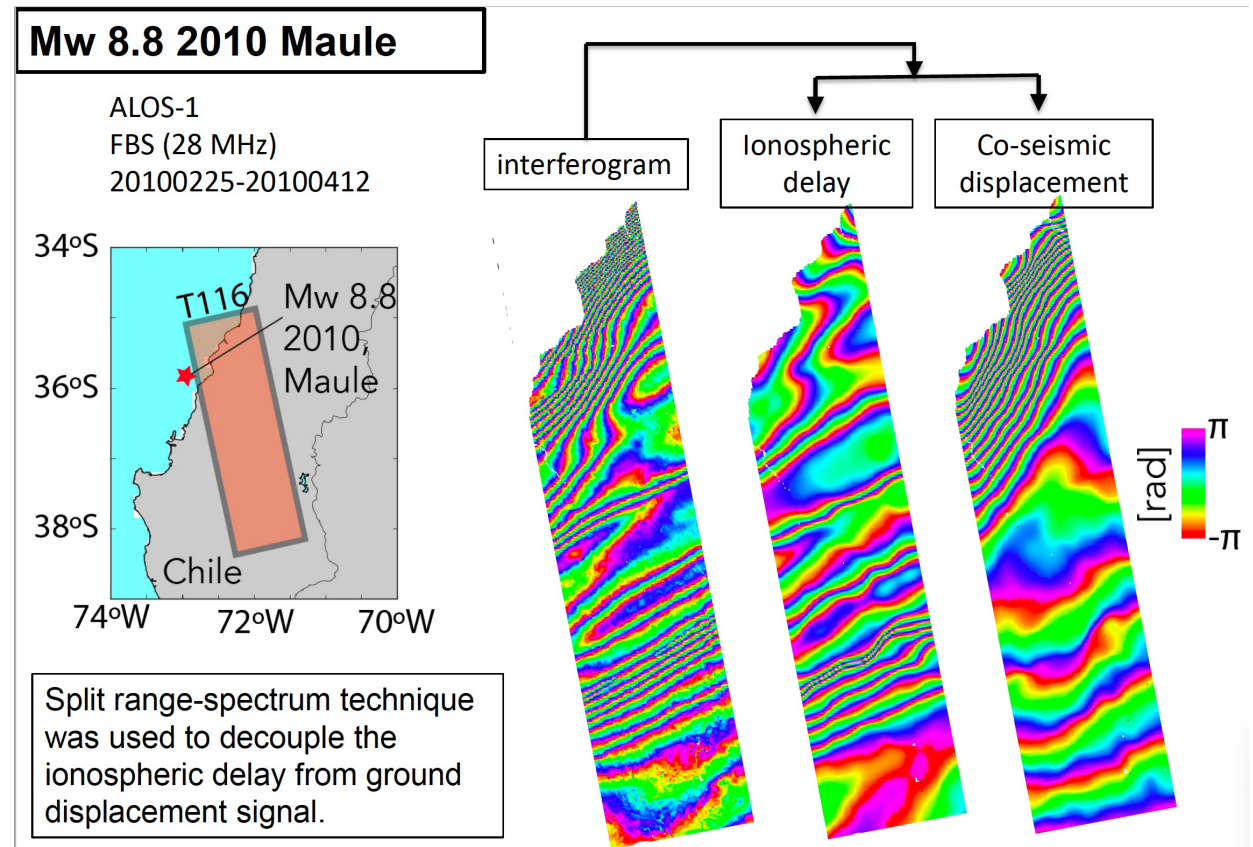


Ionospheric phase estimation

Ionosphere is a dispersive media with respect to microwave signal

Ionosphere impacts SAR data in all different frequencies. However the effect is larger in low frequencies (e.g., P and L bands compared to high frequencies such as X and C bands)

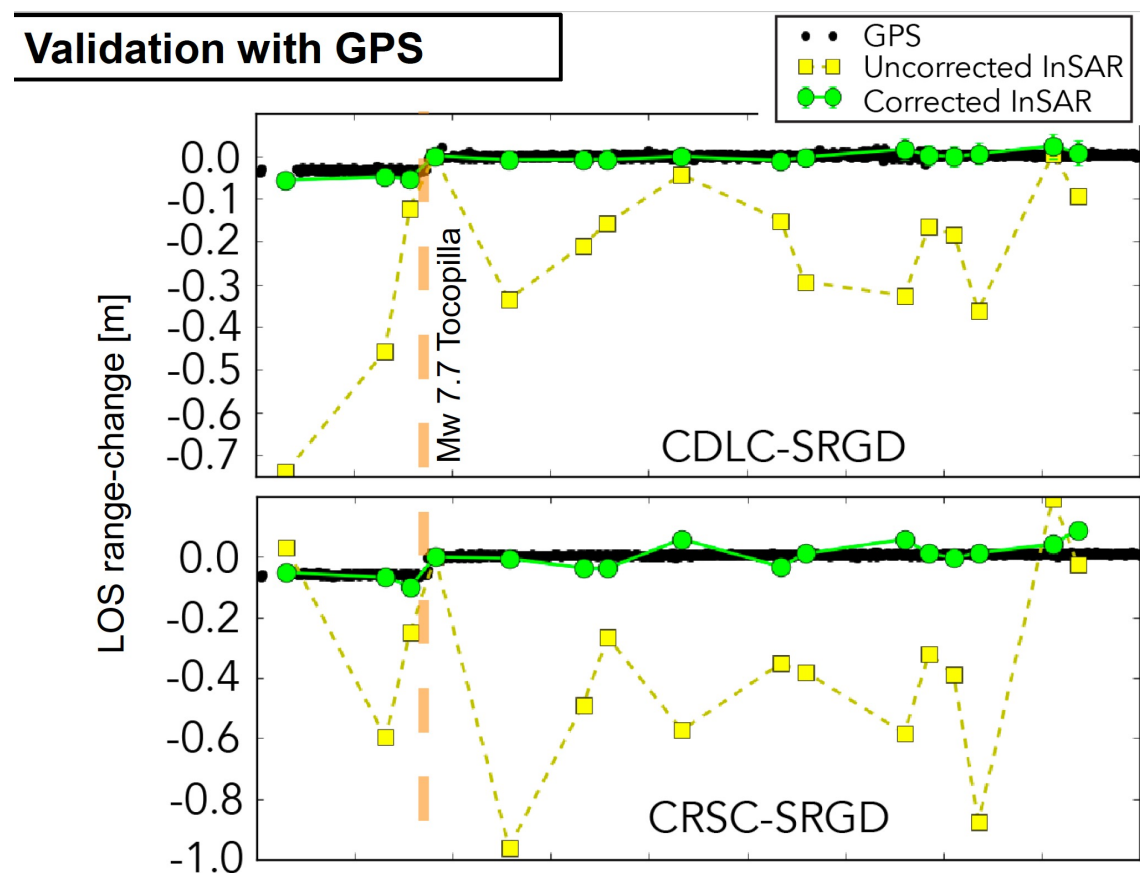
The dispersive nature of ionosphere provides an opportunity to estimate the ionospheric delay from SAR data



Impact of ionospheric phase on InSAR time-series

The InSAR time-series before and after ionosphere correction compared with GNSS time-series demonstrates the impact of ionospheric phase on InSAR time-series in L-band.

The impact of ionosphere is smaller in higher frequency radar data, however several studies have demonstrated that the ionosphere contribution is not negligible in C-band data.



Fattahi et al 2017

jpl.nasa.gov

Towards operational InSAR time-series

- ❑ Current and future major SAR missions provide global SAR SLC products
- ❑ Some future SAR missions (e.g., NISAR) plans to produce interferograms
- ❑ Continental scale ground displacement time-series products are being developed over different regions:
 - European displacement map is released
 - OPERA project is funded to develop InSAR displacement time-series over most parts of North America
- ❑ Big InSAR displacement time-series data will be available to monitor and mitigate hazards and to better understand physical processes that cause surface displacement

References

Mirzaee, Amelung, Fattahi, Nonlinear phase-linking using joint permanent and distributed scatterers, Computers and Geosciences, (in review) 2022

Fattahi and Amelung, DEM error correction in InSAR time-series, IEEE-TGRS
<https://ieeexplore.ieee.org/abstract/document/6423275>

Yunjun, Fattahi, Amelung, 2019, “Small baseline InSAR time series analysis: Unwrapping error correction and noise reduction”, Computer and Geoscience,
<https://www.sciencedirect.com/science/article/pii/S0098300419304194>

Zheng, Fattahi, Agram, Simons, Rosen,
On Closure Phase and Systematic Bias in Multilooked SAR Interferometry, IEEE TGRS
<https://ieeexplore.ieee.org/abstract/document/9758802>

Ferretti, Fumagalli, Novali, Prati, Rocca and Rucci, A New Algorithm for Processing Interferometric Data-Stacks: SqueeSAR, IEEE-TGRS
<https://ieeexplore.ieee.org/abstract/document/5765671>

Ansari, DeZan, Bamler, Sequential Estimator: Towards Efficient InSAR Time-series, IEEE-TGRS
<https://ieeexplore.ieee.org/abstract/document/8024151>

Ansari, DeZan, Parizzi, Study of Systematic Bias in Measuring Surface Deformation With SAR Interferometry,
<https://ieeexplore.ieee.org/abstract/document/9130052>

Open source software

ISCE2

<https://github.com/isce-framework/isce2>

ISCE3

<https://github.com/isce-framework/isce3>

Mintpy

<https://github.com/insarlab/MintPy>

FRInGE

<https://github.com/isce-framework/fringe>

MiaplPy

<https://github.com/insarlab/MiaplPy>